

OPTICS CORRECTION AND LOW EMITTANCE TUNING AT THE PHASE 1 COMMISSIONING OF SuperKEKB

Y. Ohnishi*, Y. Funakoshi, H. Koiso, A. Morita, K. Oide, and H. Sugimoto
KEK, Tsukuba, Japan

Abstract

The SuperKEKB collider has finally come to the first commissioning, Phase 1 without the final focus system and before Belle II detector roll-in. In order to accomplish an extremely high luminosity of $8 \times 10^{35} \text{ cm}^{-2} \text{ s}^{-1}$, the nano-beam scheme is adopted. Since the vertical emittance is one of the keys in this scheme, optics corrections for low emittance tuning are applied. The non-interleaved sextupole scheme is utilized in the arc section. Skew quadrupole-like corrector is equipped for each sextupole. These skew quadrupole-like correctors can correct both X-Y coupling and physical vertical dispersions which induce the vertical emittance. Beta function and physical horizontal dispersion are corrected by fudge factors of quadrupoles and/or horizontal orbit bumps at the sextupoles. Overall optics performance as well as the strategy of low emittance tuning is also presented.

Table 1: Machine Parameters in Phase-1 (Without Intra-beam Scattering)

| | LER | HER | Unit |
|-----------------|-----------------------|-----------------------|------|
| E | 4.000 | 7.007 | GeV |
| I | 1.01 | 0.87 | A |
| n_b | 1576 | | |
| ε_x | 1.8 | 4.6 | nm |
| α_p | 2.45×10^{-4} | 4.44×10^{-4} | |
| σ_δ | 7.52×10^{-4} | 6.30×10^{-4} | |
| V_{RF} | 7.56 | 12.61 | MV |
| σ_z | 4.6 | 5.3 | mm |
| ν_s | -0.0192 | -0.0253 | |
| ν_x | 44.53 | 45.53 | |
| ν_y | 46.57 | 43.57 | |
| U_0 | 1.76 | 2.43 | MeV |
| τ_x | 46 | 58 | msec |

INTRODUCTION

The SuperKEKB collider [1] is an asymmetric-energy and a double-ring electron-positron collider. The energy of the electron ring is 7 GeV(HER) and the positron ring is 4 GeV(LER). The collision point is one and the circumference is 3 km. The target luminosity is $8 \times 10^{35} \text{ cm}^{-2} \text{ s}^{-1}$, which is 40 times as high as the predecessor KEKB collider [2]. In order to accomplish the extremely high luminosity, a nano-beam scheme [3] is adopted.

There are three stages for the commissioning of SuperKEKB; Phase-1, Phase-2, and Phase-3. The initial commissioning was done during Phase-1 without the final focus system before Belle II roll-in. The Phase-1 commissioning was started in February 2016 and operated until the end of June 2016 for about 5 months. The commissioning for Phase-2 will start in November 2017 and will operate for 5 months with the final focus system and Belle II detector. The first collision will be performed in Phase-2, however, the vertex detector will not be installed. The physics run with the full detector in Phase-3 will start October 2018, then the luminosity will increase gradually by squeezing the beta function at the IP and increasing the beam currents toward the target luminosity.

The vertical emittance is one of the most important issues in Phase-1 since the luminosity performance significantly depends on the coupling parameter in the nano-beam scheme. Table 1 shows machine parameters in Phase-1.

OPTICS MEASUREMENTS AND CORRECTIONS

The lattice for Phase-1 is the same lattice as those of Phase-2 and Phase-3 except for the interaction region(IR). Since there is no final focus magnet in the vicinity of the IP, the field strengths of quadrupole magnets in the IR are adjusted so as to connect the arc lattice. The optics tuning [4] without the final focus, the solenoid field, and the local chromaticity corrections can be performed for Phase-1. The lattice designs of the so-called interaction region in the LER and the HER are shown in Fig. 1.

The optical functions such as beta functions, dispersions, and X-Y couplings were measured and corrected in the LER and HER, respectively. The beta functions are obtained by orbit responses induced by six kinds of dipole correctors for each x and y direction [5]. The physical dispersions are measured by orbit displacements for the rf frequency shifts between -500 Hz and +500 Hz. Note that the dispersions are physical and different from normal mode dispersions. In the case of the X-Y couplings, vertical leakage orbits from horizontal orbits induced by six kinds of horizontal dipole correctors are used to correct the X-Y couplings instead of four X-Y coupling parameters of $r_1 - r_4$. The number of BPMs is 438 in the LER and 460 in the HER to measure closed orbits. The BPM gain mapping and the beam based alignment(BBA) have been performed before the optics tuning.

In order to correct the beta functions, the measured beta functions and phase-advance are compared with those calculated by the reference optics and amount of the correc-

* yukiyoshi.ohnishi@kek.jp

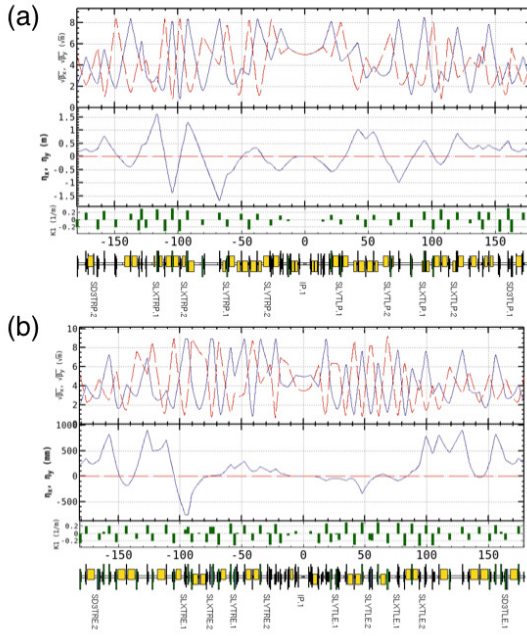


Figure 1: Lattice Design of “Interaction Region” in Phase-1; (a) LER and (b) HER.

tion of field strength for each quadrupole magnets are estimated. Correction coils are installed for each quadrupole magnet, however, the correction was performed by families of quadrupole magnets during the Phase-1 commissioning. The arc lattice adopts non-interleaved sextupole correction scheme and two identical sextupoles are connected by $-I'$ transfer matrix. The dispersions and X-Y couplings are corrected by using this specialty. The horizontal dispersions are corrected by using asymmetric local bumps in the horizontal direction at pairs of two horizontal focusing sextupoles(SF). The horizontal offset of the sextupole generates quadrupole field, however, this quadrupole field is localized between two identical sextupoles then only horizontal dispersions can be corrected. The vertical dispersions and the X-Y couplings are corrected by using skew quadrupole-like correctors at the sextupole magnets. The opposite sign of the skew quadrupole field can correct only the vertical dispersions, on the other hand, the same sign can correct only the X-Y couplings. Because of the non-interleaved sextupole scheme, the corrections of vertical physical dispersions and X-Y couplings can be solved independently for each other.

Table 2 shows the results of optics corrections. After these optics corrections, the vertical emittance has achieved 8 pm in the LER which was measured by an X-ray beam size monitor. The vertical emittance is derived by $\varepsilon_y = \sigma_y^2/\beta_y$. Figure 2 shows the history of the vertical emittance and the vertical physical dispersion in the LER. In another way, the vertical emittance can be estimated by measured optical functions and magnet configurations;

$$\varepsilon_y = C_q \gamma^2 \frac{I_{5,y}}{I_2}. \quad (1)$$

The normal dispersions can be derived by X-Y coupling parameters and transfer matrix between neighboring two BPMs in the model. The vertical emittance of 8 pm in the LER is obtained by this estimation which is consistent with the X-ray measurement. On the other hand, the measured vertical beam size in the HER was $30 \mu\text{m}$ for $\beta_y = 7.6 \text{ m}$ without any corrections, which corresponds to the vertical emittance of 40 pm when corrections for the X-ray measurement was applied. This value seems to be too large because the optics tuning is the same level between the LER and HER as shown in Table 2. A simulation assuming a mis-alignment of the sextupoles which reproduces the measured optical functions provides the vertical emittance of 5 – 20 pm. We consider that the calibration issues of X-ray monitor still remains. The vertical emittance is indirectly estimated to be 6 pm by using the measured optical functions in the HER.

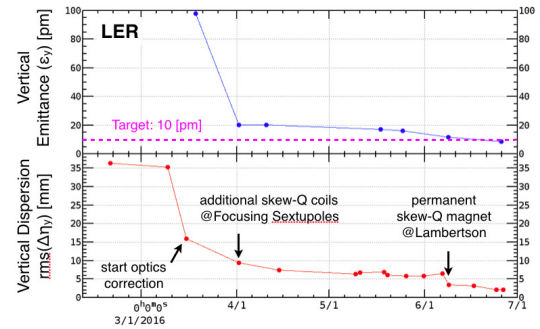


Figure 2: History of Vertical Emittance and Vertical Physical Dispersion in the LER.

Table 2: Results of the Optics Tuning in Phase-1. X-Y coupling* refers an average value of $\text{rms}(\Delta y)/\text{rms}(\Delta x)$ induced by six kinds of horizontal dipole correctors. Dispersions are physical variables in the table.

| Items | Symbol | LER | HER |
|-----------------------|---|-------|-------|
| Coupling strength | $ C^- (\times 10^{-3})$ | 1.2 | 2.0 |
| X-Y coupling* | $\text{rms}(\Delta y)/\text{rms}(\Delta x)$ | 0.9 % | 0.6 % |
| Hor. dispersion | $\text{rms}(\Delta \eta_x)$ | 8 mm | 11 mm |
| Ver. dispersion | $\text{rms}(\Delta \eta_y)$ | 2 mm | 2 mm |
| Hor. β function | $\text{rms}(\Delta \beta_x/\beta_x)$ | 3 % | 3 % |
| Ver. β function | $\text{rms}(\Delta \beta_y/\beta_y)$ | 3 % | 3 % |
| Hor. tune | $\Delta \nu_x (\times 10^{-4})$ | 2 | 5 |
| Ver. tune | $\Delta \nu_y (\times 10^{-4})$ | 5 | 1 |

OFF-MOMENTUM OPTICS

The dynamic aperture for a particle without a momentum deviation is almost recovered by the optics correction when machine errors decrease the dynamic aperture. However, the dynamic aperture with momentum deviations decreases compared with the ideal lattice even though the optics correction is performed. It is necessary to correct the

off-momentum optics in order to recover the dynamic aperture. The optical parameters, a chromatic phase-advance and a chromatic X-Y coupling are expected to be useful to accomplish this purpose. The chromatic phase-advance is adjusted by using sextupole magnets. The chromatic phase-advance in the horizontal and the vertical direction are expressed as

$$\chi_i(x) = \frac{1}{2\pi} \frac{\partial \Delta\psi_{x,i}}{\partial \delta} \quad (2)$$

$$\chi_i(y) = \frac{1}{2\pi} \frac{\partial \Delta\psi_{y,i}}{\partial \delta}, \quad (3)$$

where

$$\Delta\psi_{x,i} = \psi_{x,i} - \psi_{x,i-1} \quad (4)$$

$$\Delta\psi_{y,i} = \psi_{y,i} - \psi_{y,i-1}. \quad (5)$$

The number of locations is about 450 for each ring which corresponds to the neighboring BPMs. In order to correct the chromatic phase-advance, the field gradient of the sextupole magnets, ΔK_2 , are obtained by solving these equations:

$$\begin{pmatrix} \chi_{1,m}(x) - \chi_{1,d}(x) \\ \vdots \\ \chi_{N,m}(x) - \chi_{N,d}(x) \\ \chi_{1,m}(y) - \chi_{1,d}(y) \\ \vdots \\ \chi_{N,m}(y) - \chi_{N,d}(y) \\ \xi_{x,m} - \xi_{x,d} \\ \xi_{y,m} - \xi_{y,d} \end{pmatrix} = M_{resp} \begin{pmatrix} \Delta K_{2,1}/K_{2,1} \\ \Delta K_{2,2}/K_{2,2} \\ \vdots \\ \Delta K_{2,M}/K_{2,M} \end{pmatrix}, \quad (6)$$

where m indicates the measurements, d indicates the model calculation, M_{resp} is a response matrix calculated by the model lattice, N is the number of BPMs, and M is the number of families of the sextupole magnets. In the Phase-1 commissioning, M is 50. The measurements of the phase advance for each momentum deviations are similar to the beta measurement with the frequency shift between -500 Hz and +500 Hz. The corrections for the sextupole families in the LER are shown in Fig. 3. The field gradient, K_2 , which corresponds to the rated current for the defocusing sextupole(SD) is -8.2 1/m^2 and 5.0 1/m^2 for the focusing sextupole(SF). The amount of the sextupole correction is within 5 % of the rated current.

Figure 4 (a) shows the chromatic phase-advance before the correction and Fig. 4 (b) shows after the correction in the LER. The blue plots indicate the measured values and the green plots indicate the model calculations. The motivation of analysis for the off-momentum optics comes from the discrepancy of the chromaticity between measurements and the model lattice. Table 3 shows the measured chromaticity and calculated values by using the model lattice in the LER. The betatron tunes as a function of the momentum deviations, δ , are also shown in Fig. 5.

Although the phase advance and the beta function are derived by the model independent, one of the Twiss parameters, $\alpha_{X,y}$ is obtained by using a transfer matrix between

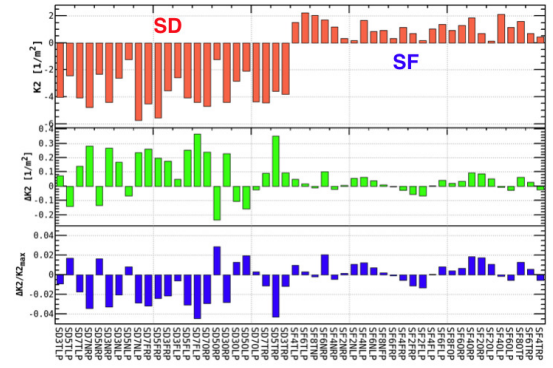


Figure 3: Corrections for the Field Gradient of the Sextupole Families in the LER.

Table 3: Chromaticity in the LER.

| Symbol | Meas. | Model before | Model after |
|---------|-------|--------------|-------------|
| ξ_x | 2.97 | 0.87 | 3.00 |
| ξ_y | 1.88 | 5.78 | 2.15 |

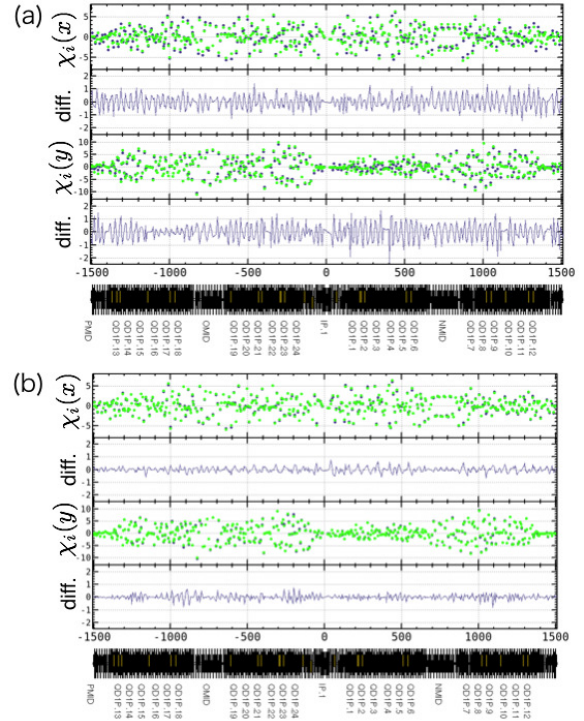


Figure 4: Chromatic Phase-Advance in the LER; (a) Before Correction and (b) After Correction. Measurements(blue) and Model(green).

neighboring two BPMs with the model and measured β functions and phase advances. The chromatic functions, $W_{X,y}$ can be defined by

$$W_{x,y} = \sqrt{\left(\frac{1}{\beta_{x,y}} \frac{\partial \beta_{x,y}}{\partial \delta} \right)^2 + \left(\frac{\partial \alpha_{x,y}}{\partial \delta} - \frac{\alpha_{x,y}}{\beta_{x,y}} \frac{\partial \beta_{x,y}}{\partial \delta} \right)^2}. \quad (7)$$

Figure 6 shows the chromatic functions for the measurements and the model after the correction in the LER. The

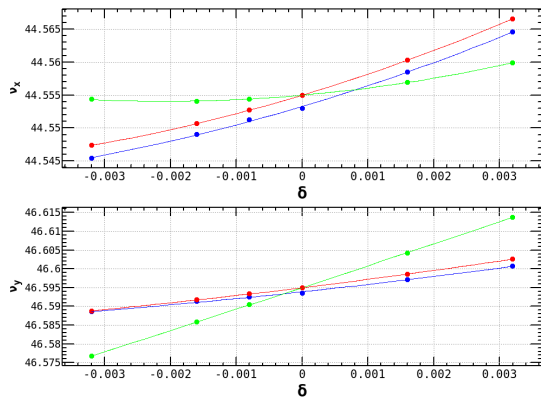


Figure 5: Chromaticity in the LER. Measurement(blue), Model before correction(green), Model after correction(red)

chromatic functions calculated by the model lattice can also reproduce the measured chromatic functions well after the correction in the LER.

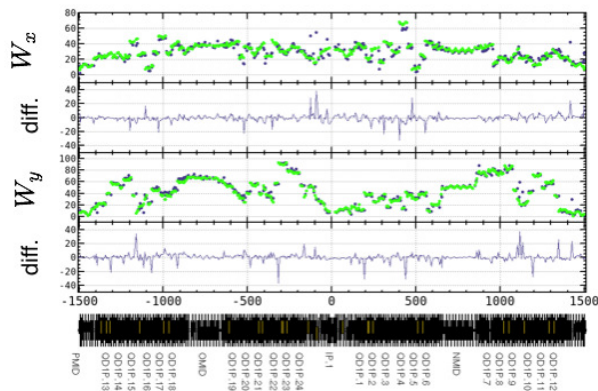


Figure 6: $W_{x,y}$ Function in the LER. Measurements(blue) and Model(green) after Correction.

CONCLUSIONS

The optics measurements and corrections have successfully been worked during Phase-1. The vertical emittance of 8 pm has been achieved in the LER which is smaller than the tentative target value at this stage. The value of the vertical emittance measured by X-ray beam-size monitor and the estimation from the measured optical functions are consistent with each other in the LER. However, the vertical emittance in the HER is still discrepancy between the X-ray measurement and the estimation from the optical functions. The reason is under study so far.

The analysis of the off-momentum optics has been performed. Understanding of the off-momentum optics is necessary to optimize the dynamic aperture. Measurements of the chromatic phase-advance and the correction of the field gradient for the sextupole magnets are presented. The correction of the sextupole magnets is less than 5% of the rated current. Consequently, the chromatic phase-advance, chromaticity, and the chromatic functions, $W_{x,y}$, can be adjusted on the model lattice.

REFERENCES

- [1] Y. Ohnishi *et al.*, *Prog. Theor. Exp. Phys.* 2013 03A011 (2013).
- [2] T. Abe *et al.*, *Prog. Theor. Exp. Phys.* 2013 03A001 (2013).
- [3] “SuperB Conceptual Design Report”, INFN/AE-07/2, SLAC-R-856, LAL 07-15, March 2007.
- [4] Y. Ohnishi *et al.*, in *Proceedings of IPAC2016*, Busan, Korea, May (2016), paper THPOR007.
- [5] A. Morita *et al.*, *Phys. Rev. ST-AB*, vol. 10, p. 072801, 2007.